EARTHQUAKE ENGINEERING AND STRUCTURAL DYNAMICS
Earthquake Engng Struct. Dyn. 2003; **32**:1291–1311 (DOI: 10.1002/eqe.275)

Design of yielding metallic and friction dampers for optimal seismic performance

L. M. Moreschi*,† and M. P. Singh

Department of Engineering Science and Mechanics, Virginia Tech, Blacksburg, VA 24061, U.S.A.

SUMMARY

This paper deals with the optimal design of yielding metallic dampers and friction dampers together as they both have similar design characteristics and parameters. Ample tests and analytical studies have confirmed the effectiveness of these energy dissipation devices for seismic response control and protection of building structures. Since these devices are strongly non-linear with several parameters controlling their behaviour, their current design procedures are usually cumbersome and not optimal. In this paper, a methodology is presented to determine the optimal design parameters for the devices installed at different locations in a building for a desired performance objective. For a yielding metallic damper, the design parameters of interest are the device yield level, device stiffness, and brace stiffness. For a friction device, the parameters are the slip load level and brace stiffness. Since the devices and the structures installed with these devices behave in a highly non-linearly manner, and thus must be evaluated by a step-by-step time history approach, the genetic algorithm is used to obtain the globally optimal solution. This optimal search approach allows an unusual flexibility in the choice of performance objectives. For demonstration purposes, several sets of numerical examples of optimal damper designs with different performance objectives are presented. Copyright © 2003 John Wiley & Sons, Ltd.

1. INTRODUCTION

The effectiveness of energy dissipation devices, such as yielding metallic dampers and friction dampers, is now well recognized for reducing the dynamic response of civil structures exposed to seismic environment. Among the yielding metallic devices, the added damping and stiffness (ADAS) [1, 2] and triangular-plate added damping and stiffness (TADAS) [3] are quite popular in seismic applications. Similarly, friction dampers with different designs have been proposed and used in practice [4–7]. These devices can accommodate a large dissipation of energy through yielding of the steel or through friction at the two sliding surfaces. For a given excitation intensity, the level of force at which the device would yield or slip

* Correspondence to: M. P. Singh, Department of Engineering Science and Mechanics, Virginia Tech, Blacksburg, VA 24061, U.S.A.
† Current address: Bechtel Power Corp., Frederick, MD, U.S.A.
‡ E-mail: mpsingh@vt.edu

Contract/grant sponsor: National Science Foundation; contract/grant number: CMS9626850 and CMS9987469.

Received 25 September 2001
Accepted 23 September 2002

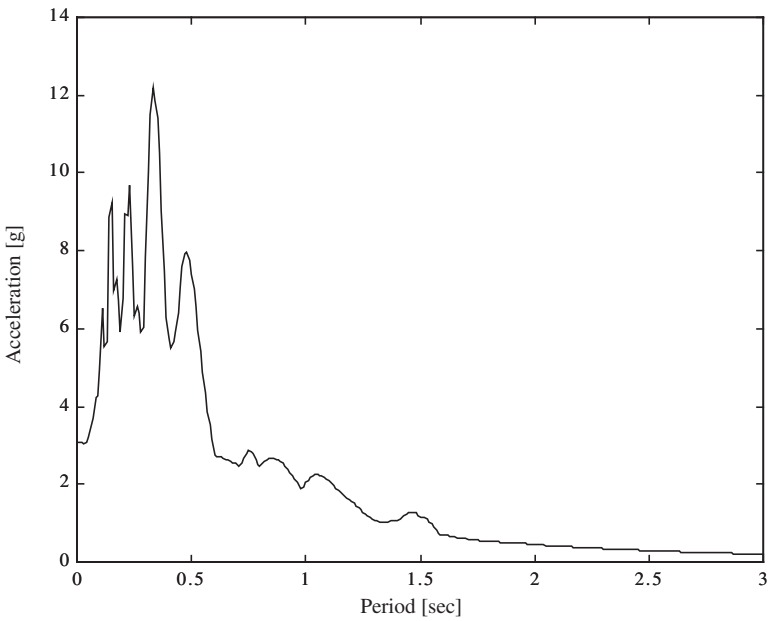

Figure 1. San Fernando earthquake pseudo-acceleration response spectrum for 3% damping.

determines the energy that is likely to be dissipated. Thus, at a low level of excitation a yielding or friction device may not provide any dissipation of energy. Also, depending upon where the device is installed in a structure, it may or may not participate in the dissipation of energy. The determination of the most appropriate yielding level or slip load level at different placement locations in the structure is, thus, an important design issue which must be resolved for effective utilization of these devices in practice. This paper deals with the optimal selection of the design parameters of yielding metallic and friction damping systems, installed at different locations in a building structure, to achieve a prescribed performance objective.

The installation of such hysteretic dampers in a structure would render it to behave nonlinearly even if all other structural members were designed to remain linear. Therefore, the analysis of structures installed with these devices must be done by a step-by-step time history analysis. To determine the optimal design parameters of these devices with such nonlinear time history analysis is an involved problem. Perhaps, one can attempt to use a gradient based optimization scheme to determine optimal design parameters. Such an approach has been successfully used with linear systems [8]. However, these techniques may lead to a locally optimal solution near the starting design guess, especially if several such solutions exist. This can be appreciated by an inspection of a simple acceleration response spectrum curve depicted in Figure 1 for a ground motion time history. For this simple example of a single degree of freedom system, if one were to use a gradient-based approach to obtain the optimum values of the system parameters (say, the system stiffness and damping ratio within a practical range) that would minimize the response for this motion, the search procedure would surely get trapped in one of the valleys near the initial design guess. If the globally optimal

solution is desired then several randomly selected initial guesses must be used. Moreover, the additional information required by the search procedure, such as the calculations of the gradients of the objective functions and constraints can be cumbersome for nonlinear systems. In addition, the force–deformation relationships of these devices may introduce discontinuities in the gradient functions depending on the model used to characterize their hysteretic cyclic behaviour. Therefore, the implementation of these approaches for optimal design with highly non-linear energy dissipation devices can be a difficult task.

In this paper, the use of genetic algorithms is advocated for the optimal design of such highly non-linear devices with hysteretic force deformation characteristics. The formulation of the optimization-based approach is first presented along with a brief description of the selected optimization technique. The mechanical parameters governing the behaviour of the devices are then identified. For demonstration purposes, an analytically convenient hysteretic model is adopted for response calculations of the combined structural system. The approach, however, can be used with any model. Non-linear step-by-step time history analyses are carried out for performance evaluations of the system. The optimal numerical results for a number of alternative performance indices are presented.

PROBLEM DEFINITION

The equations of motion of an N degree of freedom building structure with supplemental energy dissipation devices subjected to a ground excitations at its base can be written in the following standard form:

$$\mathbf{M}\ddot{\mathbf{u}}(t) + \mathbf{C}_s\dot{\mathbf{u}}(t) + \mathbf{K}_s\mathbf{u}(t) + \sum_{d=1}^{n_l} \mathbf{r}_d P_d(t) = -\mathbf{M}\mathbf{E}\ddot{X}_g(t) \tag{1}$$

where $\mathbf{M}, \mathbf{K}_s$ and $\mathbf{C}_s$ represent, respectively, the $N \times N$ mass, structural stiffness and inherent structural damping matrices; $\ddot{X}_g(t)$ is the seismic excitation; $\mathbf{E}$ is the vector of ground motion influence coefficients; $\mathbf{u}(t)$ is the N-dimensional relative displacement vector with respect to the base, and a dot over a symbol indicates differentiation with respect to time. The local force $P_d(t)$ due to a passive damper installed at the dth location is considered through the N-dimensional influence vector $\mathbf{r}_d$, with n_l being the number of possible locations for a device in the structure. A general expression for the passive force P_d applied by an energy dissipation device considered in this study can be defined by a differential operator as

$$P_d[d_1, \ldots, d_n, h_d(t), \Delta_d(t), \dot{\Delta}_d(t), t] = 0 \tag{2}$$

where d_i represents the mechanical parameters characterizing the behaviour of the devices, $h_d(t)$ is an internal variable of the element, and $\Delta_d(t)$ the local deformations of the device element. The local device deformation and the deformations rate $\dot{\Delta}_d(t)$ are related to those of the main structure by

$$\Delta_d(t) = \mathbf{r}_d^T\mathbf{u}(t); \quad \dot{\Delta}_d(t) = \mathbf{r}_d^T\dot{\mathbf{u}}(t) \tag{3}$$

It is noted that the effectiveness of these protective systems in improving the seismic performance of a structure is a function of several variables such as their number, their location in the structure, and their physical parameters. To obtain an acceptable design and arrangement,

one could start by assuming a reasonable placement pattern for the devices and then vary their parameters until the structural system meets the performance requirements. However, as the structure becomes more complex and the number of protective devices increases such an approach may not be efficient or practical for design purposes.

In this study, the problem of determining the best design parameters of hysteretic dampers is posed as an optimization problem. The intent is to fully exploit the energy dissipation capability of each device while providing the best response reduction. The effectiveness of a given distribution of the devices, and their chosen properties, can be measured in terms of a properly selected performance function or index. The objective may be to minimize or maximize such a function. Such a design problem could be expressed in terms of an optimality criterion as follows:

$$\underset{\mathbf{d}}{\text{minimize}} \quad f[\mathbf{R}(\mathbf{d},t)]; \quad t \in [0,t_f] \tag{4}$$

$$\text{subject to} \quad g_j(\mathbf{d},t) \leqslant 0 \quad j=1,\ldots,m; \quad t \in [0,t_f] \tag{5}$$

where $\mathbf{R}(\mathbf{d},t)$ is the desired structural response vector in terms of which the performance function $f(-)$ is defined, $\mathbf{d}$ is the vector of the design variables representing the parameters of the added damping elements, and m is the number of inequality constraints g_j which may include the upper and lower bounds on the design variables.

A number of alternate performance indices can be used to evaluate the seismic performance of a building structure. Depending upon the chosen criteria, different design solutions will be obtained. Moreover, a design solution obtained by reducing some measure of the structural response may increase some other response quantities. It is, thus, clear that there is no unique way of defining an optimal problem; the choice depends on the performance objectives. In this paper, several forms of performance indices are used to demonstrate the optimal design procedure.

As mentioned earlier, genetic algorithms are quite well suited for solving problems such as the one stated by Equations (4) and (5). These algorithms are robust search and optimization techniques. They are based on the principles of natural biological evolution where stronger individuals are likely to be the winners in a competing environment [9, 10]. Genetic algorithms explore the design space by operating on a population of potential solutions (designs). The process tries to simulate the biological evolution by means of random genetic changes that produce successively better approximations to a design solution. Since many design points are considered simultaneously in the search space, genetic algorithms have a reduced chance of converging to local optima. Moreover, they do not require any computations of gradients of complex functions to guide their search; the only information needed is the response of the system to calculate the objective or fitness function. This approach has been effectively used in several earlier studies, a few of which are cited here [11–17].

DESIGN PARAMETERS OF HYSTERETIC DEVICES

The force–deformation behaviour of the yielding dampers and friction dampers has some common characteristics. Therefore, we describe first the modelling of metallic devices and then

specialize it for friction devices. The force–deformation response under arbitrary cyclic loading of the hysteretic devices has often been approximated by discrete multi-linear models, such as the elasto-perfectly plastic model and the bilinear model. More comprehensive and accurate models have also been devised to represent more accurately the constitutive behaviour of these devices [18]. To facilitate the identification of the parameters involved in the design of a typical damper, here a simple bi-linear hysteretic force–deformation model is used. Figure 2(a) represents the bay of a structural frame installed with an added hysteretic damper. Herein, the combination of a damper and the brace members that support the device is called as the device–brace assembly. The design parameters of interest of such an assembly are the yield displacement and stiffness of the device, and the stiffness of the brace on which the device is supported. For a given stiffness of the building storey where the device is installed, the yield force P_y can be related to the device parameters as follows [19, 20]:

$$P_y = k_d \Delta_{yd} = \mathrm{SR} k_s \left(1 + \frac{1}{\mathrm{B/D}}\right) \Delta_{y_d} \tag{6}$$

where k_s is the storey stiffness, Δ_{yd} is the yield displacement, $\mathrm{B/D} = k_b/k_d$ is the ratio of the brace stiffness k_b to the device stiffness k_d, and $\mathrm{SR} = k_{bd}/k_s$ is the ratio of the assembly stiffness k_{bd} to storey stiffness k_s. The combined stiffness of device–brace assembly, schematically shown in Figure 2(b) and 2(c), can be expressed in terms of the device stiffness k_d and the bracing stiffness k_b as

$$k_{bd} = \frac{1}{(1/k_b) + (1/k_d)} = \frac{k_d}{1 + (1/(\mathrm{B/D}))} \tag{7}$$

In this study, it is assumed that the bracing members as well as the main structural members are designed to remain elastic during an earthquake, and the stiffness coefficient k_d of the device used in Equation (7) corresponds to the initial elastic values of the yielding elements.

Equation (6) expresses the basic relationship between the parameters of the assumed bilinear model. From this equation, it can be observed that in a given structure (i.e. k_s known) the behaviour of a hysteretic element is governed by the four key parameters: the yield load P_y, the yield displacement of the device Δ_{yd}, and the stiffness ratios SR and B/D. However, only three of these variables are independent since the fourth one can be determined from Equation (6).

A relationship similar to Equation (6) can also be developed for friction dampers. For these dampers, the stiffness k_d of the device can be considered as infinitely large, i.e. $k_d \approx \infty$ for a classical hysteresis loop of the friction dampers (See Figure 3(a)). With this, the stiffness k_{bd} of the device assemblage becomes the same as the stiffness k_b of the supporting brace. That is,

$$k_{bd} = k_b; \quad \mathrm{SR} = \frac{k_b}{k_s} \tag{8}$$

As shown in Figure 3(b), the yield or slip load can then be related to the deformation Δ_y experienced by the device–brace assembly as

$$P_s = k_{bd}\, \Delta_y = k_b\, \Delta_y \tag{9}$$

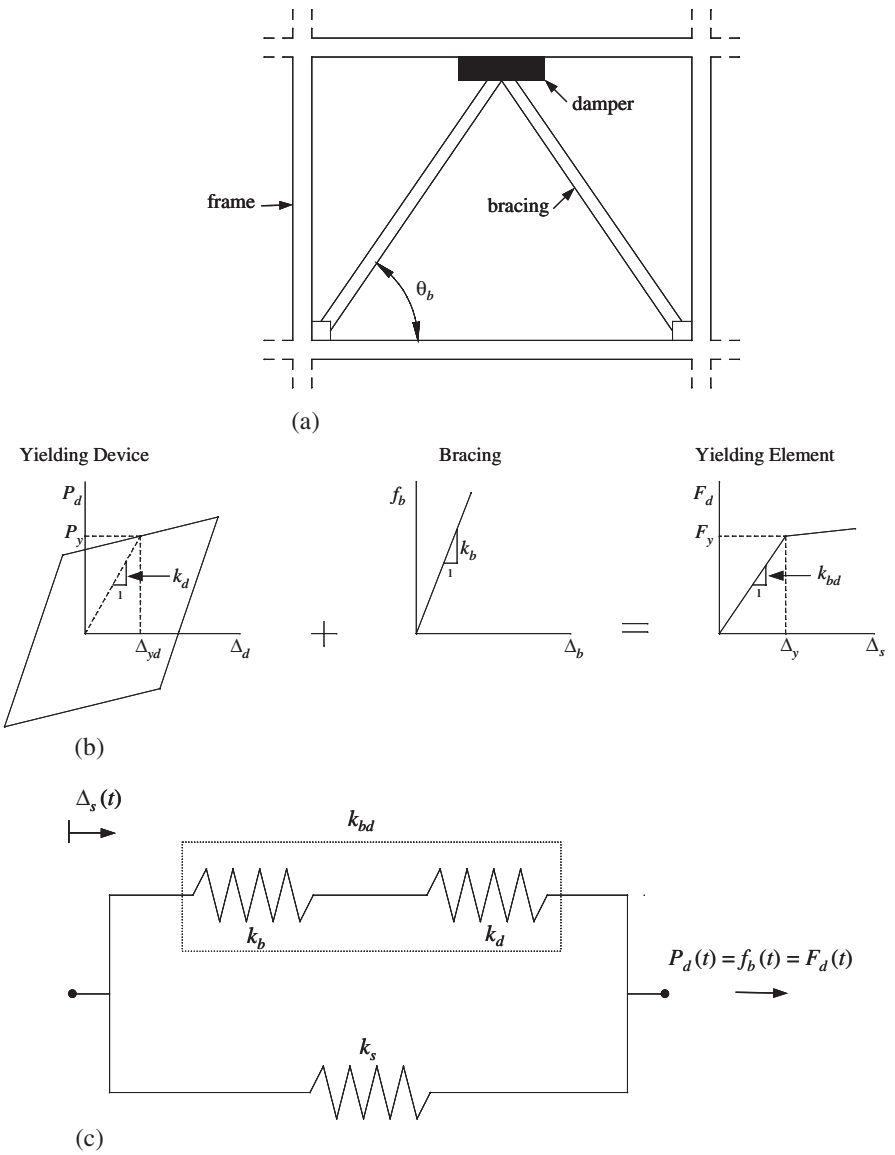

Figure 2. Yielding metallic damper, (a) typical configuration, (b) yielding metallic device, bracing and yielding element parameters, (c) stiffness properties of device-bracing assembly.

For design purposes, this equation can be expressed in terms of the stiffness parameter SR using Equation (8) in Equation (9) as

$$P_s = \mathrm{SR} k_s \Delta_y \tag{10}$$

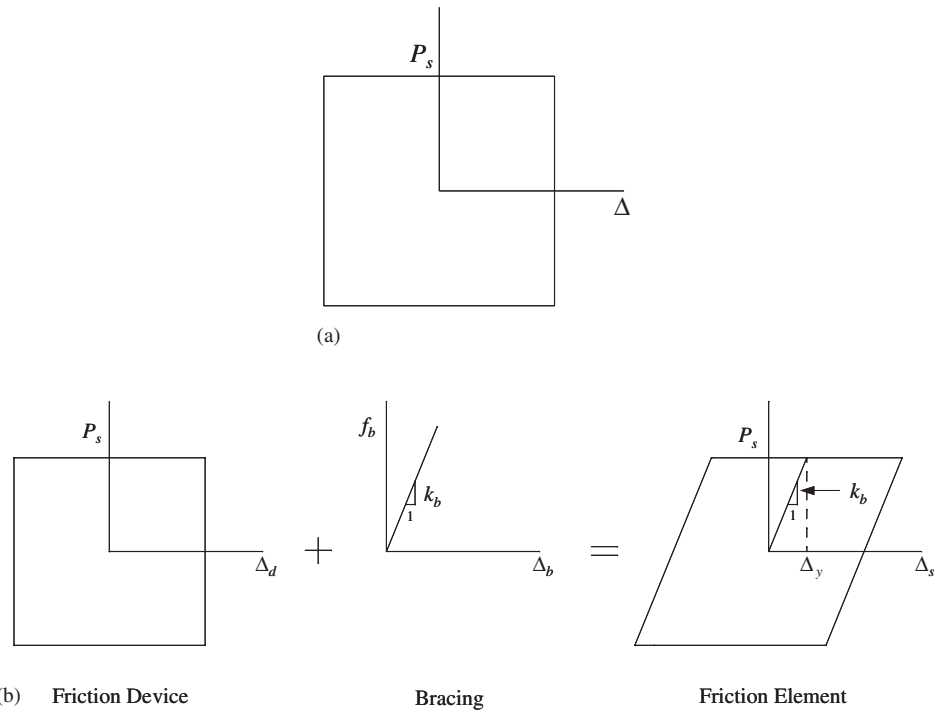

Figure 3. Idealized hysteretic behavior of friction dampers, (a) friction device on rigid bracing, (b) friction device mounted on flexible support.

Equation (10) is the basic expression relating the mechanical parameters of a friction element. From this, it is noted that the behaviour of a friction element is governed by the slip load P_s, the stiffness ratio SR, and the displacement of the brace Δ_y at which the device starts to slip. However, only two of these variables are independent since the third one can be determined from Equation (10).

HYSTERETIC MODELS AND SYSTEM EQUATIONS

A bilinear model was considered in the above discussion, primarily to facilitate the identification of the basic design variables and relationship between them. Models that are more comprehensive have also been proposed [18] that accurately capture the subtleties of the force deformation characteristics. They certainly can be used with the formulation and the optimization approach to be used herein, with additional numerical effort. When performing time history analyses, however, the numerical complications may arise even in simpler bi-linear models due to the sharp transitions from the inelastic to elastic states during the loading, unloading, and reloading cycles. The presence of such abrupt changes in stiffness requires the use of numerical procedures that can locate these transition points in order to avoid erroneous results. As the number of devices installed in a building structure increases and as the

different phase or stiffness transition conditions for each device must be taken into account in the numerical calculations, the bilinear representation of the devices can become computationally inefficient. Herein, therefore, to simplify the computations in this study a continuous Bouc–Wen's model [21] is used to characterize the hysteretic force–deformation characteristic of the dampers. It is realized that this model has its shortcomings, but it still offers a practically convenient representation of the force–deformation characteristics which captures the essence of the hysteretic behaviour. An especially attractive feature of the Bouc–Wen's model is that the same equation governs the behaviour in the different stages of the inelastic cyclic response of the device. Moreover, since this model is in the form of a differential equation, it can be conveniently coupled with the equations that describe the motion of the building structure.

In this model, the restoring force, $P_{\mathrm{d}}(t)$, developed in the dth device–brace assembly is expressed by the following equations:

$$P_{\mathrm{d}}(t) = \mathrm{SR}_{\mathrm{d}} k_{\mathrm{s}}^{d} [\alpha \Delta_{\mathrm{d}}(t) + (1-\alpha)\Delta_{\mathrm{y}}^{d} h_{\mathrm{d}}(t)] \tag{11}$$

$$\Delta_{\mathrm{y}}^{\mathrm{d}} \dot{h}_{\mathrm{d}}(t) - \dot{\Delta}_{\mathrm{d}}(t) + \gamma |\dot{\Delta}_{\mathrm{d}}| h_{\mathrm{d}}(t) |h_{\mathrm{d}}(t)|^{\eta-1} + \beta \dot{\Delta}_{\mathrm{d}} |h_{\mathrm{d}}(t)|^{\eta} = 0 \tag{12}$$

where, $h_{\mathrm{d}}(t)$ is a dimensionless auxiliary variable that has hysteretic characteristics; $\Delta_{\mathrm{y}}^{\mathrm{d}}$ is the yielding displacement of the dth device–brace assembly, $k_{\mathrm{s}}^{\mathrm{d}}$ denotes the stiffness of the storey in which the element is located, and α, γ, β and η are the model parameters. These values must be chosen to calibrate the predicted response of the hysteretic element with the one obtained experimentally. Figure 4 shows the hysteresis loops generated by the Bouc–Wen's model for exponent values of $\eta = 1, 5$ and 25 when subjected to a sinusoidal excitation. The values of $\alpha = 0.02, \eta = 25, \beta = 0.1$, and $\gamma = 0.9$ have been selected in this study to characterize the hysteretic behaviour of the metallic device–brace assembly.

Expressions (11) and (12) for the element forces, when combined with the equations of motion (1), can be rewritten as a set of first-order differential equations of the following form:

$$\begin{Bmatrix} \ddot{\mathbf{x}}(t) \\ \dot{\mathbf{x}}(t) \\ \dot{\mathbf{h}}(t) \end{Bmatrix} = g[\mathbf{x}(t), \dot{\mathbf{x}}(t), \mathbf{h}(t), \ddot{X}_{\mathrm{g}}(t), t] \tag{13}$$

The differential equation (13) constitutes a set of three coupled non-linear differential equations. In their explicit forms, these equations are as follows:

$$\ddot{\mathbf{x}}(t) = -\mathbf{M}^{-1} \left[\mathbf{C}_{\mathrm{s}} \dot{\mathbf{x}}(t) + \left(\mathbf{K}_{\mathrm{s}} + \alpha \sum_{d=1}^{n_l} \mathbf{r}_{\mathrm{d}}\, \mathrm{SR}_{\mathrm{d}} k_{\mathrm{s}}^{d}\, \mathbf{r}_{\mathrm{d}}^{\mathrm{T}} \right) \mathbf{x}(t) + (1-\alpha) \sum_{d=1}^{n_l} \mathbf{r}_{\mathrm{d}} \mathrm{SR}_{\mathrm{d}} k_{\mathrm{s}}^{d} \Delta_{\mathrm{y}}^{d} h_{\mathrm{d}}(t) \right]$$
$$- \mathbf{E} \ddot{X}_{\mathbf{g}}(t)$$
$$\dot{\mathbf{x}}(t) = \dot{\mathbf{x}}(t)$$
$$\dot{h}_{\mathrm{d}}(t) = \frac{1}{\Delta_{\mathrm{y}}^{d}} [\mathbf{r}_{\mathrm{d}}^{\mathrm{T}} \dot{\mathbf{x}}(t) - \gamma |\mathbf{r}_{\mathrm{d}}^{\mathrm{T}} \dot{\mathbf{x}}(t)| h_{\mathrm{d}}(t) |h_{\mathrm{d}}(t)|^{\eta-1} - \beta \mathbf{r}_{\mathrm{d}}^{\mathrm{T}} \dot{\mathbf{x}}(t) |h_{\mathrm{d}}(t)|^{\eta}]; \quad d = 1, \ldots, n_l \tag{14}$$

These equations can be integrated using several accurate and efficient solvers.

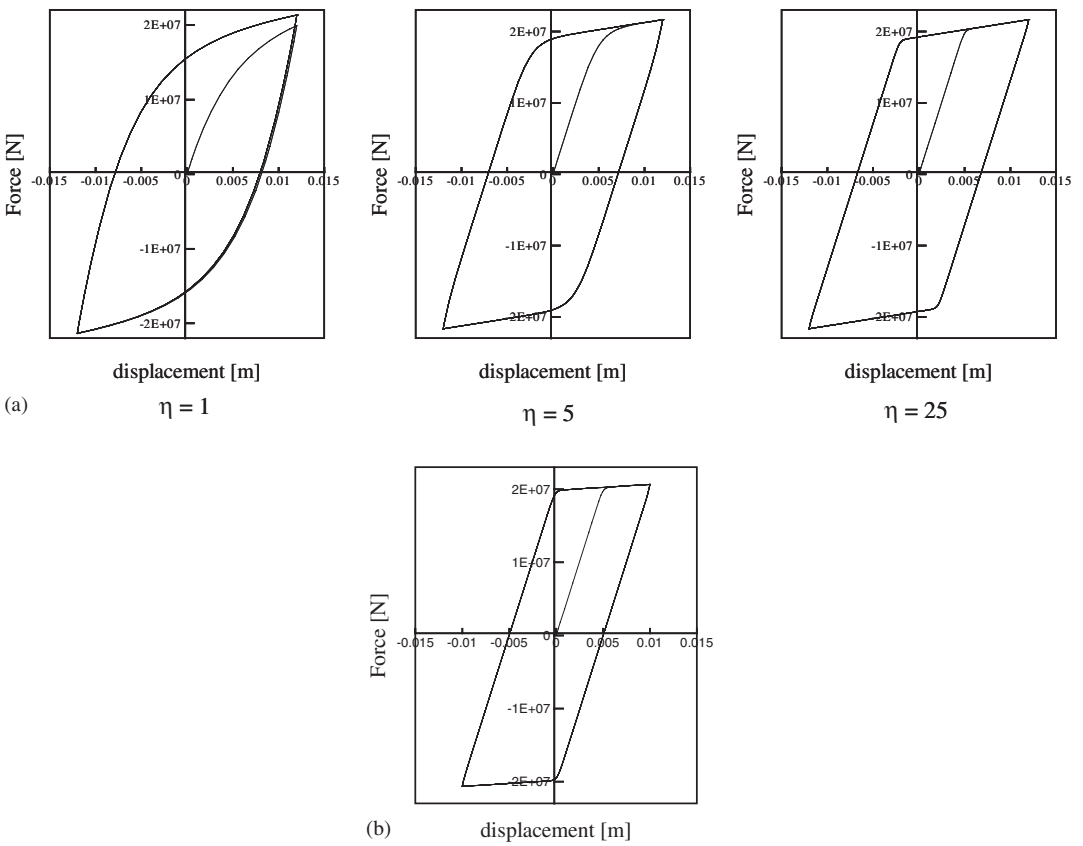

Figure 4. Hysteresis loops generated by the Bouc–Wen's model under sinusoidal excitation, (a) exponent values $\eta = 1, 5$ and 25 ($\gamma = 0.9,\ \beta = 0.1,\ \alpha = 0.05,\ \mathrm{H} = 1,\ \Delta_y = 0.005\,\mathrm{m}$), (b) model used in this study ($\eta = 25,\ \gamma = 0.9,\ \beta = 0.1,\ \alpha = 0.02,\ \mathrm{H} = 1$).

The hysteretic behaviour of the friction element can also be effectively represented by a continuous Bouc–Wen's model. Recognizing the absence of any post-yielding or strain-hardening effect, the force $P_{\mathrm{d}}(t)$ developed in a friction element can be obtained from Equation (11) in terms of the slip load at the element P_{s}^{d} and the hysteretic variable $h_{\mathrm{d}}(t)$ as

$$P_{\mathrm{d}}(t) = P_{\mathrm{s}}^{d} h_{\mathrm{d}}(t) \tag{15}$$

$$P_{\mathrm{s}}^{d}\dot{h}_{\mathrm{d}}(t) - \mathrm{SR}_{\mathrm{d}} k_{\mathrm{s}}^{d}[\dot{\Delta}_{\mathrm{d}}(t) - \gamma|\dot{\Delta}_{\mathrm{d}}|h_{\mathrm{d}}(t)|h_{\mathrm{d}}(t)|^{\eta-1} - \beta\dot{\Delta}_{\mathrm{d}}|h_{\mathrm{d}}(t)|^{\eta}] = 0 \tag{16}$$

As before, the model parameters γ, β and η are adjusted to approximate the shape of the hysteresis loops. A value of $\eta = 2,\ \gamma + \beta = (\beta = 0.1, \gamma = 0.9)$ have been proposed in the literature to produce hysteresis loops of friction force versus sliding displacement that are in good agreement with experimental results [22]. For these parameters values, Figure 5(a) shows the hysteresis loop generated by the Bouc–Wen's model for different combinations of excitation frequencies and amplitudes. If the flexibility of the bracing is included in the analysis, the

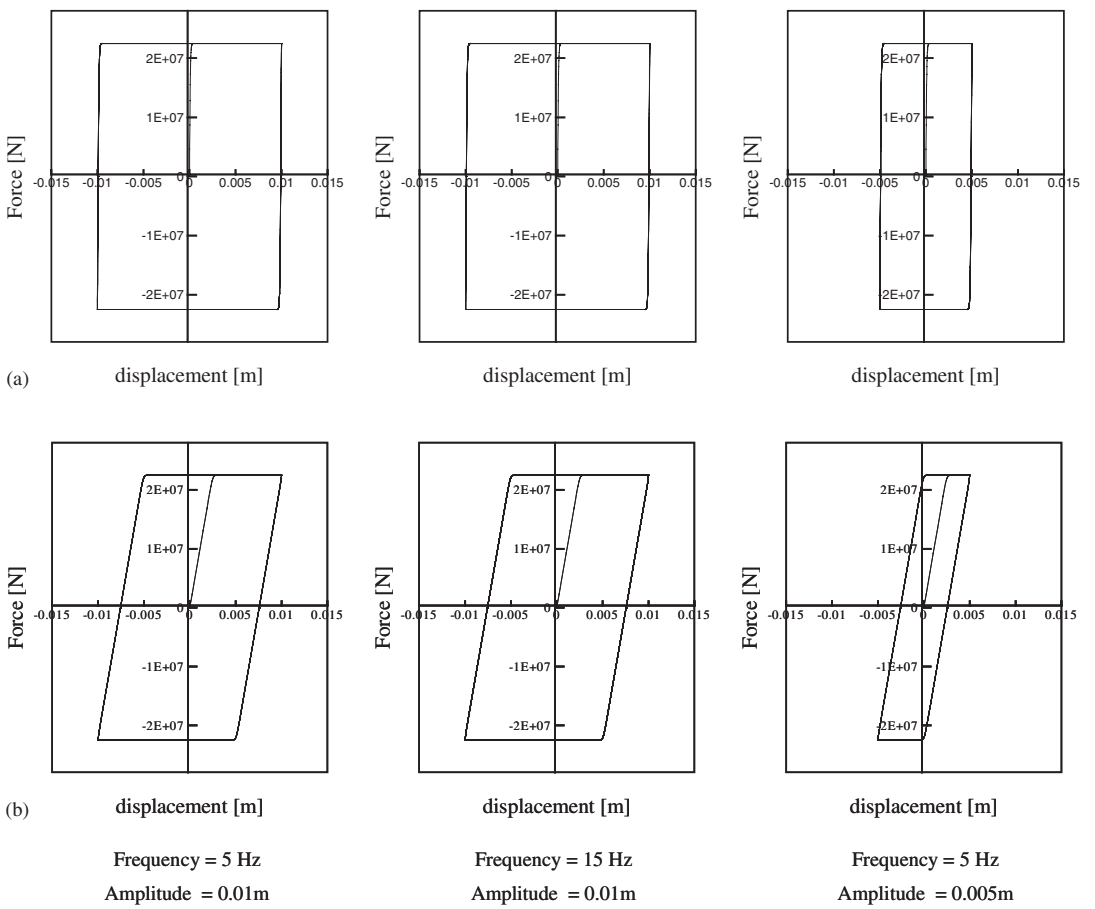

Figure 5. Hysteresis loops for the Bouc–Wen's model under sinusoidal excitation for different values of excitation frequencies and deformation amplitudes, (a) rigid bracings, ($\gamma = 0.9,\ \beta = 0.1,\ \eta = 2,\ H = 1$), (b) flexible bracings ($\gamma = 0.9,\ \beta = 0.1,\ \eta = 25,\ H = 1$).

hysteretic loop of the friction assemblage is better approximated by using an exponent coefficient $\eta = 25$, as shown in Figure 5(b).

Equations (15) and (16) along with the equations of motion can be written as a system of the first order equations (13). The three equations represented by (13) for the friction dampers are as follows:

$$\ddot{\mathbf{x}}(t) = -\mathbf{M}^{-1}\left[\mathbf{C}_s\dot{\mathbf{x}}(t) + \mathbf{K}_s\mathbf{x}(t) + \sum_{d=1}^{n_l}\mathbf{r}_d P_s^d h_d(t)\right] - \mathbf{E}\ddot{X}_g(t)$$

$$\dot{\mathbf{x}}(t) = \dot{\mathbf{x}}(t)$$

$$\dot{h}_d(t) = \frac{\mathrm{SR}_d\, k_s^d}{P_s^d}[\mathbf{r}_d^{\mathrm{T}}\dot{\mathbf{x}}(t) - \gamma|\mathbf{r}_d^{\mathrm{T}}\dot{\mathbf{x}}(t)|\, h_d(t)|h_d(t)|^{\eta-1} - \beta\mathbf{r}_d^{\mathrm{T}}\dot{\mathbf{x}}(t)|h_d(t)|^{\eta}]; \quad d = 1,\ldots,n_l \qquad (17)$$

The sets of Equations (14) and (17) have been used in the optimization study to obtain the following numerical results. In this study, these equations have been solved using the equation solver LSODA from the ODEPACK package [23].

NUMERICAL RESULTS

The numerical results are obtained for a 10-storey shear building, installed with the two types of hysteretic dampers under consideration herein. The storey stiffness varies from bottom to top with values, in the $N/m \times 10^7$ units, as: 9.26, 8.57, 7.88, 7.20, 6.51, 5.83, 5.14, 4.45, 3.77, and 3.08. The mass of each floor is 2.5×10^5 kg. The damping ratio of 3% in each mode was assumed to define the inherent energy dissipation characteristics of the structure. This damping ratio value was used to construct the damping matrix for the structure. It is assumed that there will be one device in each storey. The mechanical properties of each device can be changed independently, and will be determined by the optimization procedure. First, the results are presented for the metallic dampers followed by the results for the friction dampers.

Metallic dampers: The optimal values for the damper parameters will depend upon the choice of the desired objectives. The objective may be as simple as to reduce a single response quantity such as the base shear or acceleration of a floor. It could be also defined in terms of a composite index as a function of several response quantities. For illustration purposes, here the following performance indices have been considered for the metallic devices:

$$f_1[\mathbf{R}(\mathbf{d},t)] = \frac{1}{2}\left\{\frac{\max_i \Delta_i(t)}{\max_i \Delta_{i(o)}(t)} + \frac{\max_i[\ddot{X}_{oi}(t)]}{\max_i[\ddot{X}_{oi}(t)]}\right\} \tag{18}$$

$$f_2 = \sum_{i=1}^{n_f} \max[\ddot{X}_{oi}^2(t)] / \sum_{i=1}^{n_f} \max[\ddot{X}_{oi}^2(t)] \tag{19}$$

The index f_1 is expressed in terms of the maximum inter-storey drift and maximum floor acceleration, weighted equally. The index is expressed in a non-dimensional form using the response quantities of the original structure by using the dampers. The objective is to minimize this function by a balanced reduction of the both response quantities. The second index is expressed as the ratio of the sum of the squares of the absolute floor accelerations of the damped and undamped (original) structures. The objective of minimizing this function would be to reduce the floor accelerations.

As mentioned earlier, there are three independent parameters according to Equation (6) that need to be calculated for optimal usage of the metallic dampers. Herein, the stiffness ratio SR, yield level Δ_y, and stiffness ratio B/D are chosen as the design parameters or the design variables of interest. Since the genetic algorithms operate in the discrete design space, the design variables have to be discretized. Herein, for this, the parameter SR is considered to take on any integer value between 0 to 10. Thus, there are 11 possible choices for this variable. The value of zero corresponds to the case of no-device in the storey. The parameter B/D is also considered to take on any of the 10 possible integer values varying between 1 to 10. Based on experimental observations and suggested guidelines [19, 20], the admissible

Table I. Optimal parameters of metallic devices for the performance index F_1 of Equation (18) with different design options.

	SR		SR and Δ_{yd}			SR, Δ_{yd} and B/D			
Storey	SR_d	P_y^d (%W)	Δ_{yd} (m)	SR_d	P_y^d (%W)	Δ_{yd} (m)	SR_d	B/D_d	P_y^d (%W)
(1)	(2)	(3)	(4)	(5)	(6)	(7)	(8)	(9)	(10)
1	1.50	4.2	0.0057	1.50	4.9	0.0070	2.00	8.25	5.9
2	2.75	7.2	0.0060	3.50	11.1	0.0057	4.50	5.00	10.9
3	8.50	20.5	0.0051	5.50	13.5	0.0060	7.00	6.50	15.7
4	3.00	6.6	0.0054	7.00	16.6	0.0054	4.75	5.75	8.9
5	2.25	4.5	0.0056	3.75	8.4	0.0054	4.25	9.75	6.7
6	4.50	8.0	0.0058	3.75	7.8	0.0051	3.50	8.50	4.8
7	2.50	3.9	0.0055	5.00	8.7	0.0050	3.00	4.25	3.9
8	4.75	6.5	0.0051	6.75	9.3	0.0054	4.25	6.50	4.8
9	5.50	6.3	0.0054	6.50	8.1	0.0054	4.50	5.75	4.4
10	1.66	1.6	0.0052	3.40	3.3	0.0059	5.38	3.25	5.2
$f[\mathbf{R}(\mathbf{d}^*, t)]$	0.68			0.62			0.57		

Table II. Optimal parameters of metallic devices for the performance index F_2 of Equation (19) with different design options.

	SR		SR and Δ_{yd}			SR, Δ_{yd} and B/D			
Storey	SR_d	P_y^d (%W)	Δ_{yd} (m)	SR_d	P_y^d (%W)	Δ_{yd} (m)	SR_d	B/D_d	P_y^d (%W)
(1)	(2)	(3)	(4)	(5)	(6)	(7)	(8)	(9)	(10)
1	1.00	2.8	0.0054	1.00	3.0	0.0055	1.00	5.25	2.4
2	5.50	14.4	0.0058	7.75	23.4	0.0067	6.00	3.25	18.2
3	9.75	23.5	0.0055	9.75	26.0	0.0051	8.00	6.75	15.0
4	6.25	13.8	0.0061	7.25	19.6	0.0066	4.00	5.00	9.3
5	6.50	12.9	0.0058	4.75	10.9	0.0061	1.75	6.00	3.3
6	2.50	4.5	0.0050	3.50	6.2	0.0058	4.25	7.75	6.6
7	5.00	7.9	0.0067	3.50	7.3	0.0053	5.75	5.50	7.6
8	7.50	10.2	0.0064	7.75	13.6	0.0052	5.00	3.75	5.9
9	5.00	5.8	0.0057	7.25	9.5	0.0053	5.75	4.75	5.7
10	0.91	0.9	0.0063	3.90	4.6	0.0050	2.14	6.75	1.5
$f[\mathbf{R}(\mathbf{d}^*, t)]$	0.70			0.68			0.63		

values for the device yield level have been considered to vary between 0.005 to 0.008 m. This range has been divided into 10 equal intervals, thus providing 11 choices for this variable. Thus, for 10 possible locations of these devices on the structure, there are more than zillion possible combinations in the design space that an exhaustive search will have to explore. The genetic algorithms, however, do it very efficiently without examining each and every possibility.

The optimal parameter values obtained by genetic algorithm for the two performance indices f_1 and f_2 are shown in Tables I and II, respectively. The parameter values shown in the tables are the average of the values obtained for four synthetically generated accelerrograms. The synthetic accelerograms were generated for a Kanai–Tajimi spectral density function that was consistent with the 1994 Northridge Earthquake event [24]. The acceleration time histories were normalized to a maximum ground acceleration value of 0.45g. For the results in Columns 2 and 3, only the parameter of the stiffness ratio SR was considered to be an independent variable; the parameters of the yield level Δ_y and B/D were fixed at $\Delta_y = 0.005$ m and B/D = 2. Column 2 shows the calculated optimal stiffness ratio values SR and Column 3 the corresponding yield load calculated according to Equation (6). The last row of the table shows the performance index value of 0.68, indicating a reduction in the response of about 32%. The results in the next three columns (Columns 4–6) of the table are for the two parameters of SR and Δ_y chosen as the independent variables. The parameter B/D was fixed at a value of 2. The results in the last four columns (Columns 7–10) are for the case when all three parameters have been considered as variables. It is noted that the optimal distributions of the parameters in different stories of the building in the three cases are different. Also, the optimal values of the performance indices shown in the last row of the table indicate a continued improvement in the performance for the three cases. This improved performance can be obviously attributed to the increased flexibility gained in the design by considering more parameters as variables. Similar results were also obtained for the second performance f_2, as shown in Table II, with analogous observations.

To compare the effectiveness of the above designs based on the two performance indices in reducing other response quantities such as floor accelerations and storey shears we present Figure 6. Here we plot and compare the response values calculated for the designs with parameters given in the last four columns of Tables I and II. Also plotted are the response values for the original structure with no dissipation devices. Figure 6(a) is for acceleration response and Figure 6(b) for the storey shear responses. It is noted that the design for index f_2 is somewhat more effective in reducing the acceleration than the design for index f_1 as the former index is entirely based on the floor acceleration.

Friction dampers: Next, we present the numerical results for the optimal designs obtained for the structure installed with friction dampers. As mentioned earlier, we have three parameters in this case that are related through Equation (10). Only two of them can be chosen as independent variables. In the following, we select the parameters of the slip-load P_s and stiffness ratio SR as the two independent variables. Again, it is assumed that a single device is placed at each location. The mechanical properties of the friction elements are then determined using genetic algorithm for a specified performance index. The same 10-storey shear building and seismic motions used for the metallic dampers are used again with friction dampers.

A number of simplified procedures and design guidelines have been proposed in the literature for the determination of these parameters. In general, these design methodologies are based on the results of extensive parametric analysis [25–30]. The studies by Filiatrault and Cherry [28, 29] and Cherry and Filiatrault [30] are especially relevant. They obtained a design for a performance index, assuming that all the friction devices placed at different building locations slipped at the same threshold load $P_s^d = P_s$. Also, the same diagonal braces were used in each storey to support the devices. Under these assumptions, the design problem reduced to the determination of a single parameter—the slip-load P_s for the devices. They used an

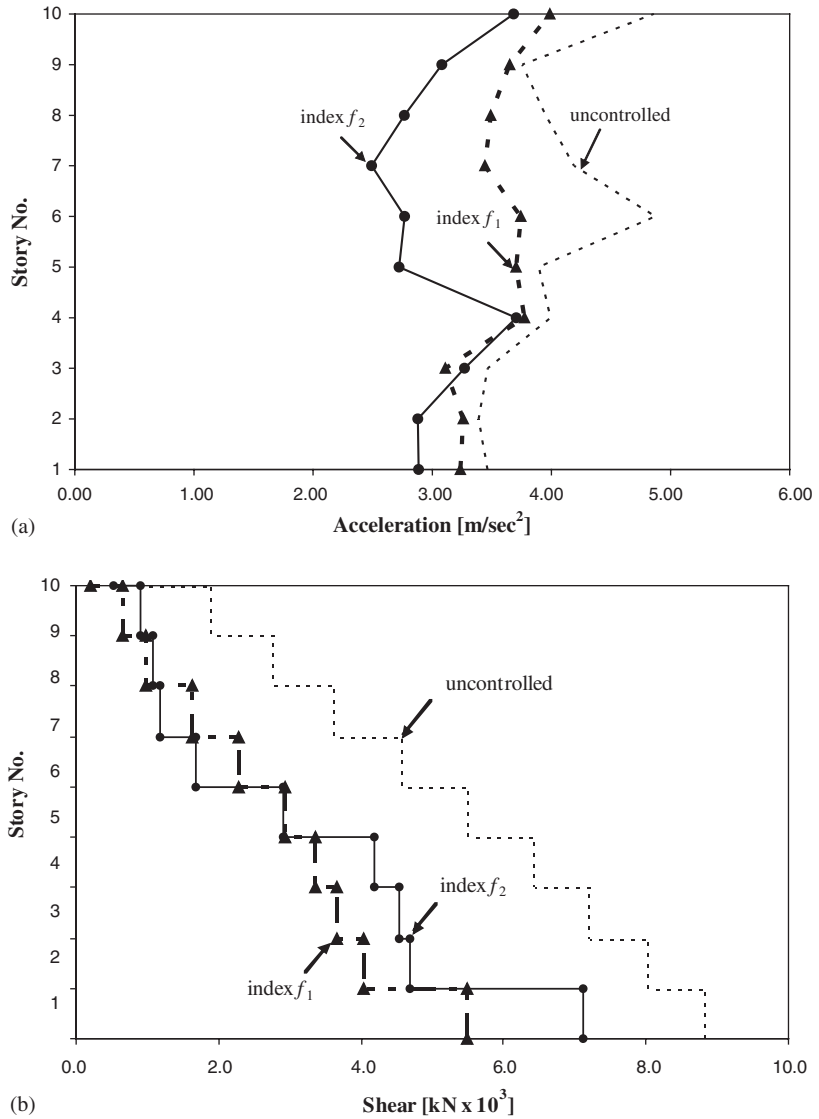

Figure 6. Comparison of maximum response quantities along the building height, (a) floor accelerations, (b) storey shears.

index called as the relative performance index (RPI) defined as follows:

$$\mathrm{RPI} = \frac{1}{2}\left(\frac{\mathrm{SEA}}{\mathrm{SEA}_{(o)}} + \frac{U_{\max}}{U_{\max(o)}}\right) \tag{20}$$

where SEA and $U_{\max}$ are, respectively, the area under the elastic strain-energy time history and the maximum strain energy for a friction-damped structure; $\mathrm{SEA}_{(o)}$ and $U_{\max(o)}$ are the

Table III. Optimal parameters of friction devices for different design options with performance index of Equation (20).

	Uniform Slip Load	Variable Slip Load	Slip load P_s^d and SR_d ratios	
Storey	P_s (%W)	P_s^d (%W)	P_s^d (%W)	SR_d
(1)	(2)	(3)	(4)	(5)
1	3.25	5.30	5.9	9.75
2	3.25	4.50	4.9	9.25
3	3.25	3.80	4.6	8.75
4	3.25	3.60	3.8	7.25
5	3.25	3.00	3.4	9.50
6	3.25	2.40	2.9	9.25
7	3.25	2.40	2.5	9.50
8	3.25	2.10	2.1	9.00
9	3.25	2.10	1.5	9.00
10	3.25	3.40	1.0	8.00
RPI	0.2681	0.2347	0.1060	

respective quantities of the original uncontrolled structure. The selection of this performance index was motivated by the direct relation that exists between the amount of elastic strain energy imparted into a building and the resulting structural response. For this simple case, Filiatrault and Cherry [29] determined the optimal slip load by a direct parametric variation analysis. A series of time-history analyses were carried out for different levels of slip-load. The value of P_s that minimized the RPI defined the optimum design parameter in the study.

Using this approach with the 10-storey structure and ground motions considered in this study, the optimal slip load for the stiffness ratio $SR = 2$ was calculated to be $0.0325W$. W is the total weight of the structure. The same optimal value was also obtained by the genetic algorithm. The corresponding RPI index was 0.2681. These results are shown in Column (2) of Table III. The design corresponding to these results will be referred to as Case I design in further discussions.

In the second case, the optimal design problem was again solved but now considering the slip-loads at each location as independent variables, denoted here as P_s^d. That is, the assumption of uniform slip-load distribution over the storey height is removed. The genetic algorithm was used to find the optimal slip load parameters in different stories that minimized the RPI. For using the genetic algorithm, the 26 possible slip load values between 0 and $0.125W$ at the intervals of $0.005W$ were considered. A value of zero for the slip load at a location means no device at the location. To compare the results for this case with the results for Case I (as well as for Case III to be discussed next), a constraint was imposed that the sum of all the slip loads at different levels in the building remain the same in the three cases. The total slip load in Case I is calculated to be 32.5% of the total weight (sum of the slip loads in Column 2, Table III). Thus, the total slip load in the other two cases was also constrained to be equal to this value. Column (3) of Table III presents the average slip-load distribution obtained using the genetic algorithm. These results have been obtained for a population of 20 individuals evolving over 500 generations. It can be noticed from the last row of Table III that for the same amount of total friction force, this optimal slip-load

distribution further reduces the RPI value by about 13%. Thus, it helped to use different slip loads at different levels. The design corresponding to the values in Column 3 will be referred to as Case II design.

In Case III, in addition to the parameter of the slip loads at different stories, the stiffness ration parameter SR_d is also set free to take any integer value between 1 and 10. Again, the genetic algorithm is used to search for the best design solution. Since the number of possible design combinations has increased, a larger population of 30 individuals has been considered for the numerical calculations. Columns 4 and 5, respectively, show, the values of the slip loads P_s^d and stiffness ratios SR_d for each storey. The total friction load in the three cases is kept the same for a comparison of the results in these cases. It is noted that the RPI index is further reduced by 60%. Such dramatic improvement in the seismic performance of the structural system can be attributed to the additional stiffness used in the optimal design as well as to a better utilization of their energy dissipation capabilities.

Figure 7 compares the force–deformation responses of the friction elements located at different building stories when the structure is subjected to the San Fernando earthquake. The results for Case I (for the uniform slip-load distribution) are shown in Figure 7(a). It is observed that the devices located at the upper stories are not slipping and consequently do not extract any energy from the system. Figure 7(b) shows the hysteresis loops for the Case III design (Columns 4 and 5 of Table III.) It is observed that in this case, all the friction elements are actively engaged in the energy dissipation.

Figure 8 compares the response reduction achieved by the Cases I and III designs in the maximum inter-storey drifts, displacements, and absolute floor accelerations. These response quantities are the average of the responses obtained for the simulated acceleration records. The Case III design is seen to be more effective than the Case I design in reducing the drift and displacement response. Case III is also more effective in reducing the top floor acceleration. However, the acceleration response is not much affected at the lower stories. Acceleration reduction can be improved by using a performance index that includes acceleration explicitly, such as the one used for yielding metallic damper, Equations (19) or (18). Table IV shows the optimal values of the two design variables, obtained by the genetic algorithm, for the performance index of Equation (18). For this design solution, Figure 9 compares the maximum inter-storey drifts, maximum displacements and maximum absolute accelerations values obtained at different stories of the original and friction-damped structures. Again, these responses are the average of the responses obtained for the ground motions used. This figure also shows the corresponding maximum responses obtained for the Case III design of the structure in Table III obtained for the RPI index. These responses quantities were previously presented in Figure 8. It seen from Figure 9 that the design solution obtained by minimizing the performance index of Equation (18) provides comparable reductions in the maximum inter-storey drifts and displacements, but better reductions in the maximum accelerations responses at all levels. Figure 10 shows the evolution of the best design in successive generations and the convergence characteristics of the genetic algorithm used in this study.

CONCLUDING REMARKS

The metallic and friction dampers can dissipate a large portion of energy in a vibration system through hysteretic cycles. They, therefore, offer attractive choices for seismic response

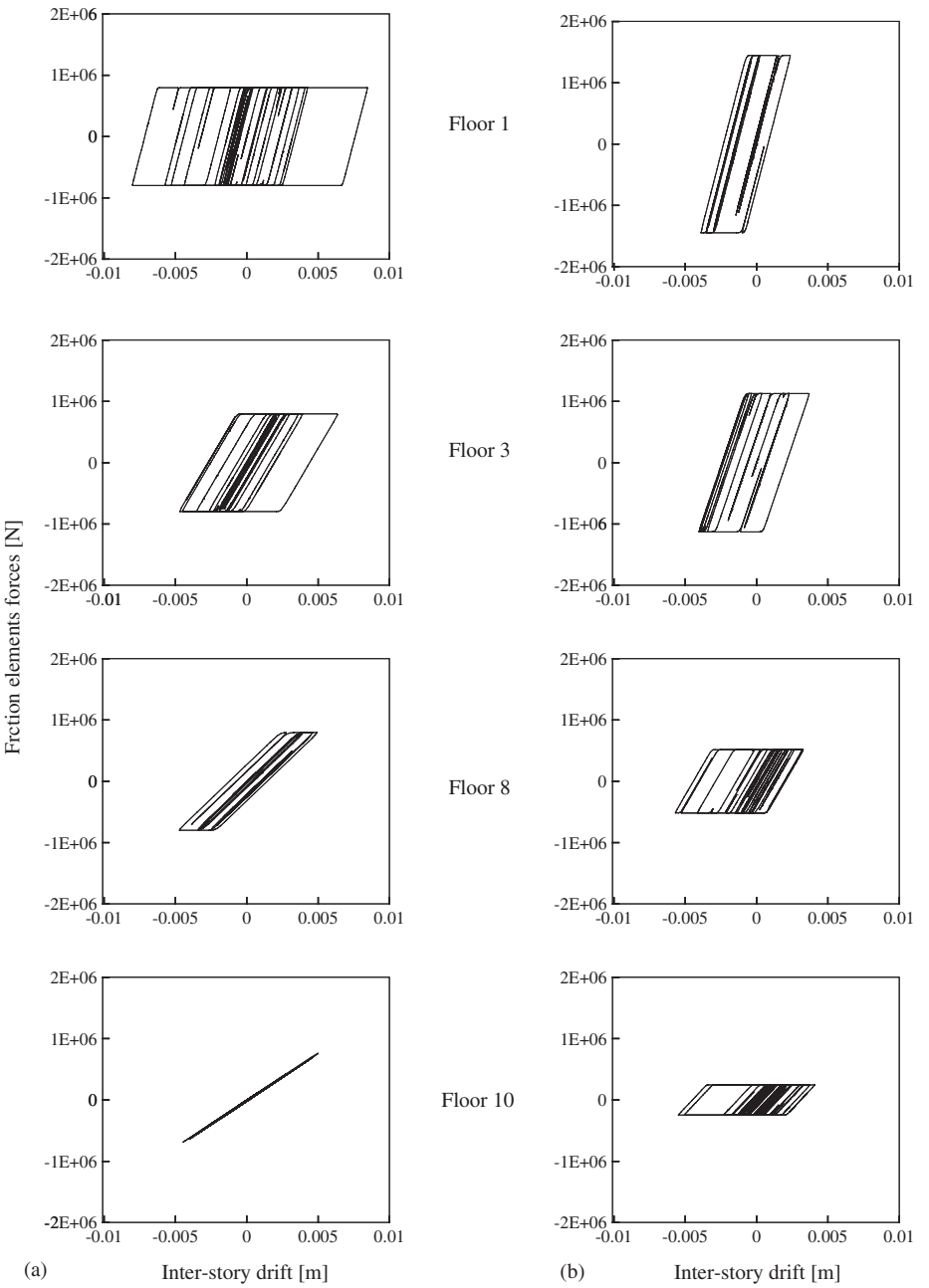

Figure 7. Comparison of force–deformation responses for friction elements obtained for the San Fernando earthquake, (a) uniform slip-load distribution, Case I, (b) genetic algorithm slip-load distribution, Case III.

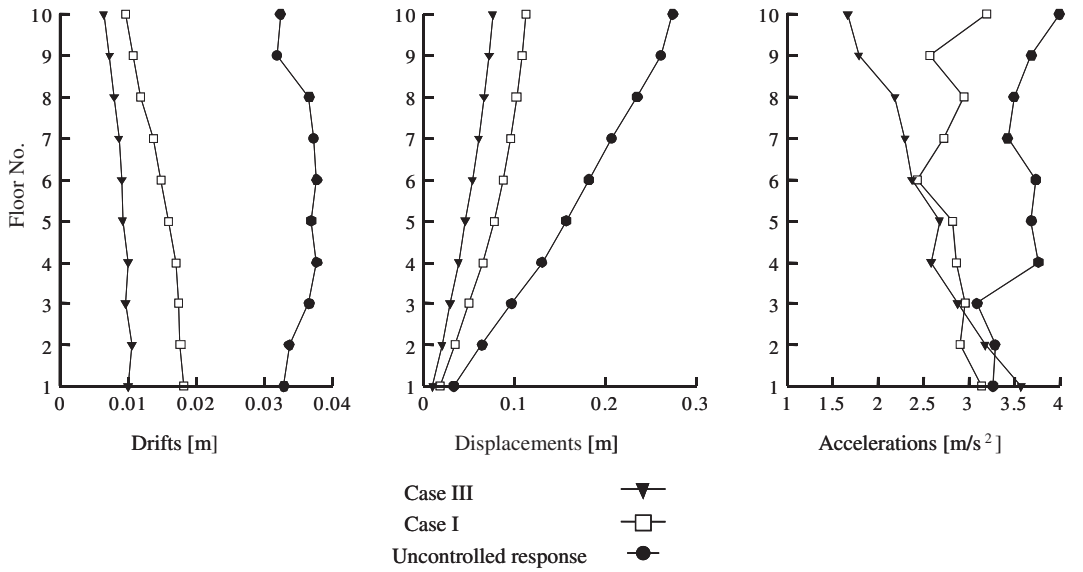

Figure 8. Comparison of maximum response quantities along the building height for the damper parameters presented in Table III for RPI index (Equation (20)).

Table IV. Optimal parameters of friction devices for the performance index of equation (18).

	Slip load P_s^d and SR_d	
Storey	SR_d	P_s^d (%W)
(1)	(4)	(5)
1	5.50	3.5
2	3.00	3.8
3	7.25	4.3
4	7.25	4.5
5	7.50	2.5
6	6.25	2.5
7	6.00	3.5
8	4.75	3.8
9	7.75	2.8
10	5.50	2.5
$f[\mathbf{R}(\mathbf{d}^*, t)]$	0.4617	

mitigation of structural systems. To evaluate the performance of a structural system installed with these devices for seismic motions, one must use a step-by-step time history analysis since these devices introduce strong non-linearities in the system. Because of this non-linearity, it is quite difficult to calculate the right design parameters of these complex systems for

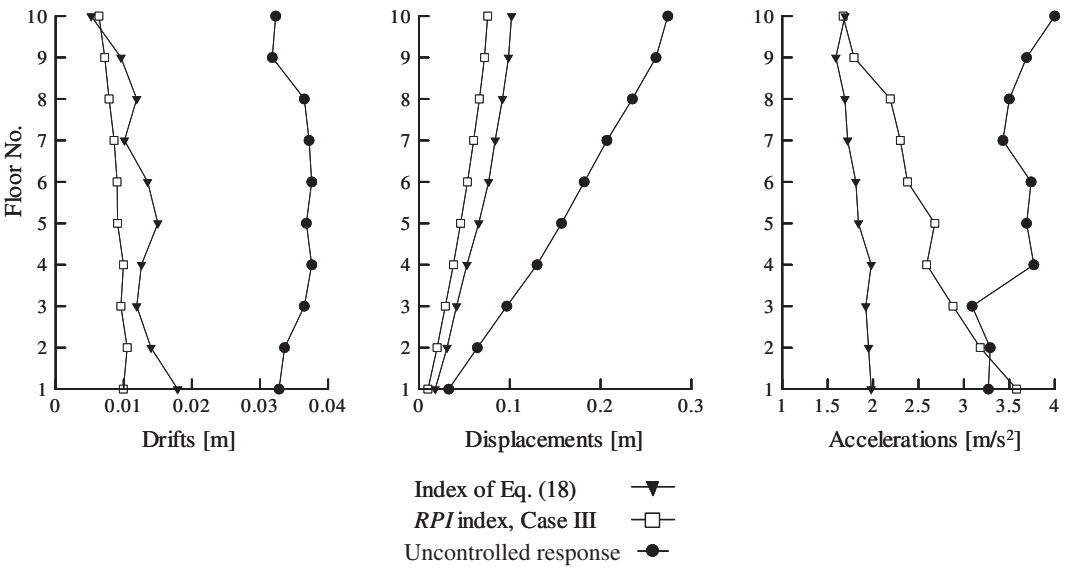

Figure 9. Comparison of maximum response quantities along the building height for the damper parameters presented in Table III for RPI index of Equation (20)) and in Table IV for index F_1 of Equation (18).

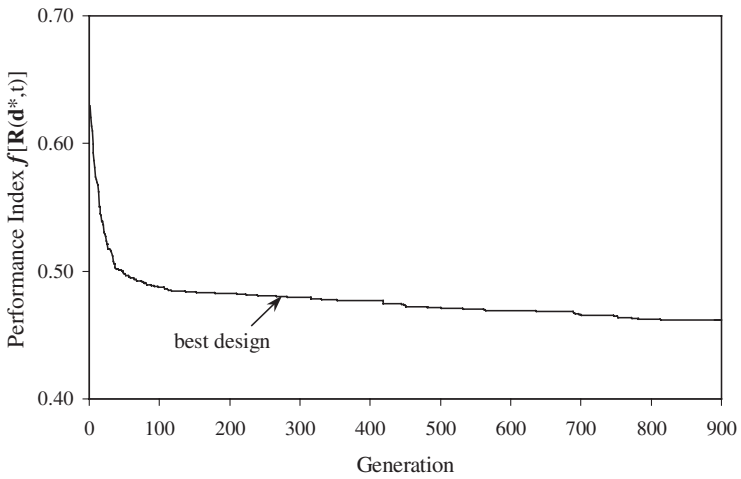

Figure 10. Optimization history for maximum response reduction using genetic algorithm.

a structural design. This study shows the design procedures of these two devices have similar characteristics. For a give structural system, the design parameters of interest for a metallic damper are the yield displacement of the device, stiffness of the device, and stiffness of the bracing that supports the device. For a friction damper, the design parameters are the slip-load

level and bracing stiffness. A method using the genetic algorithms is used to calculate the optimum choices for these parameters to satisfy a pre-selected design objective. It is shown that the possibility of varying these parameters independently of each other and at different locations of their installation in a structure provides a very desirable flexibility in the design to improve the performance. The performance objectives are defined in terms of performance functions or indices. The genetic approach offers a unusual flexibility in choosing different performance indices. Several sets of numerical results with a few different forms of performance indices are presented to demonstrate the application of the approach for selecting optimal design parameters of these complex energy dissipation systems.

ACKNOWLEDGEMENT

This study was financially supported by the National Science Foundation through grant numbers CMS-9626850 and CMS-9987469. This support is gratefully acknowledged.

REFERENCES

1. Scholl RE. Brace dampers: an alternative structural system for improving the earthquake Performance of buildings. *Proceedings of the 8th World Conference on Earthquake Engineering*, San Francisco, July 1984; 1015–1022.
2. Hanson RD. Basic concepts and potential application of supplemental mechanical damping for improving earthquake resistance. *Proceedings of the ATC seminar on Base Isolation and Passive Energy Dissipation*, San Francisco, March 1986.
3. Tsai K, Chen H, Hong C, Su Y. Design of steel triangular plate energy absorbers for seismic-resistant construction. *Earthquake Spectra* 1993; **9**(3):505–528.
4. Pall AS, Marsh C. Response of friction damped braced frames. *Journal of Structural Engineering* 1982; **108**(ST6):1313–1323.
5. Grigorian CE, Yang T, Popov EP. Slotted bolted connection energy dissipators. *Earthquake Spectra* 1993; **9**(3):491–504.
6. Nims D, Richter P, Bachman R. The use of the energy dissipating restraint for seismic hazard mitigation. *Earthquake Spectra* 1993; **9**:467–489.
7. Sumitomo Metals Industries Ltd. Friction dampers for earthquake response control. *Report* 1987; **12**.
8. Singh MP, Moreschi LM. Optimal seismic response control with dampers. *Earthquake Engineering and Structural Dynamics* 2001; **30**:553–572.
9. Holland JH. *Adaptation in Natural and Artificial Systems*. University of Michigan Press: Ann Arbor, MI, 1975.
10. Goldberg DE. *Genetic Algorithms in Search, Optimization and Machine Learning*. Addison-Wesley: Reading, MA. 1989.
11. Furuya H, Haftka RT. Placing actuators on space structures by genetic algorithms and effectiveness indices. *Structural Optimization* 1995; **9**:69–75.
12. Chan E. Optimal design of buildings structures using genetic algorithms. *Report No. EERL 97-06*, Earthquake Engineering Research Laboratory, California Institute of Technology, Pasadena, CA, 1997.
13. Cheng FY, Li D. Genetic algorithm development for multi-objective optimization of structures. *AIAA Journal* 1998; **36**(6):1105–1112.
14. Furuya O, Hamazaki H, Fujita S. Proper placement of energy absorbing devices for reduction of wind-induced vibration in high-rise buildings. *Journal of Wind Engineering and Industrial Aerodynamics* 1998; **74–76**: 931–942.
15. Hadi MN, Arfiadi Y. Optimum design of absorber for MDOF structures. *Journal of Structural Engineering* 1998; **124**:1272–1280.
16. Kim Y, Ghaboussi J. A new method of reduced order feedback control using genetic algorithms. *Earthquake Engineering and Structural Dynamics* 1999; **28**:193–212.
17. Singh MP, Singh S, Moreschi LM. Tuned mass dampers for response control of torsional buildings. *Earthquake Engineering and Structural Dynamics* 2002; **31**:749–769.
18. Soong TT, Dargush GF. *Passive Energy Dissipation Systems in Structural Engineering*. Wiley: New York, 1997.

19. Xia C, Hanson R. Influence of ADAS element parameters on building seismic response. *Journal of Structural Engineering* 1992; **118**:1903–1918.
20. Xia C, Hanson R, Wight J. A study of ADAS element parameters and their influence on earthquake response of building structures. *Report No. UMCE 90-12*, University of Michigan, Ann Arbor, MI. 1990.
21. Wen YK. Equivalent linearization of hysteretic systems under random excitation. *Journal of Applied Mechanics* (*ASME*) 1980; **47**(EM2):150–154.
22. Constantinou MC, Mokha A, Reinhorn AM. Teflon bearings in base isolation. II: Modeling. *Journal of Structural Engineering* 1990; **116**(2):455–474.
23. Hindmarsh AC. ODEPACK, A Systematized collection of ODE solvers. In *Scientific Computing*, Stepleman, RS (ed). North-Holland: Amsterdam, 1983; 55–64.
24. Lai S-SP. Statistical characterization of strong ground motions using power spectral density functions. *Bulletin of the Seismological Society of America* 1982; **72**(1):259–274.
25. Ciampi V, De Angelis M, Paolacci F. Design of yielding or friction-based dissipative bracings for seismic protection of buildings. *Engineering Structures* 1995; **17**:381–391.
26. Foti D, Bozzo L, Lopez-Almansa F. Numerical efficiency assessment of energy dissipators for seismic protection of buildings. *Earthquake Engineering and Structural Dynamics* 1998; **27**:543–556.
27. Pekau OA, Guimond R. Controlling seismic response of eccentric structures by friction dampers. *Earthquake Engineering and Structural Dynamics* 1991; **20**:505–521.
28. Filiatrault A, Cherry S. Performance evaluation of friction damped braced steel frames under simulated earthquake loads. *Earthquake Spectra* 1987; **3**:57–78.
29. Filiatrault A, Cherry S. Seismic design spectra for friction-damped structures. *Journal of Structural Engineering* 1990; **116**:1334–1355.
30. Cherry S, Filiatrault A. Seismic response control of buildings using friction dampers. *Earthquake Spectra* 1993; **9**:447–466.

